Histol Histopathol (2015) 30: 1353-1365

http://www.hh.um.es

Histology and Histopathology

Cellular and Molecular Biology

Expression of myostatin in early postnatal mouse masseter and rectus femoris muscles

Hiroshi Takada, Yoko Miwa and Iwao Sato

Department of Anatomy, School of Life Dentistry at Tokyo, The Nippon Dental University, Japan

Summary. Aims: Myostatin (Mstn) is a member of the transforming growth factor-β (TGF-β) family that inhibits muscle differentiation. In this study, we aimed to identify the relationships between Mstn, thyroid hormone receptor alpha (TRα), and myosin heavy chain (MyHC) isoform expression during early postnatal development. Methods: We investigated the expression of Mstn, TRα, and MyHCs (embryonic, slow, IIa, IIb, and IIx) using quantitative real-time RT-PCR and ELISA (Mstn) in postnatal mouse muscles between day 0 and day 10. We also examined the correlations between Mstn, TR and MyHCs during the early development of mouse masseter muscle (MM) and rectus femoris muscle (RFM). Results: Distinct Mstn mRNA expression patterns were observed in the two muscles despite nearly non-significant changes in the Mstn protein abundance in MM. The expression pattern of the TRα mRNA in the MM differed from that observed in the RFM. The expression of MyHC IIa, IIb and IIx mRNAs increased in the MM and decreased in the RFM from day 0 to day 10, whereas embryonic fiber MyHC mRNA expression was similar in both muscle types. Principal component analysis showed the existence of a correlation between: (1) TRα and MyHC, (2) Mstn and MyHC, and (3) TRα and Mstn in MM. The correlations were different in RFM and MM.

Cluster analyses identified the distinct clusters: cluster 1, days 0-4 for the MM and day 0 for the RFM; cluster 2, day 6 for the MM and day 2 for the RFM; and cluster 3, days 8-10 for the MM and days 4-10 for the RFM. Conclusions: These data suggest that TRα influences MyHC expression in both muscle types. In addition, Mstn has a limited effect in the MM related to the expression of individual MyHCs, as opposed to its role in the RFM, at early postnatal developmental stages. TRα could be involved in regulating both the temporal expression of MyHCs and Mstn at the early postnatal stages in the MM and RFM.

Key words: Myostatin, Masseter muscle, Rectus femoris muscle, Myosin, Thyroid hormone receptor, TGF-β

Offprint requests to: Dr. Iwao Sato, Department of Anatomy, School of Life Dentistry at Tokyo, The Nippon Dental University, 19-20 Fujimi, Chiyoda-ku, Tokyo 102-8159, Japan. e-mail: iwaoa1@tokyo.ndu.ac.jp

DOI: 10.14670/HH-11-631

Introduction

Myostatin (Mstn) is a transforming growth factor-β (TGF-β) family member that regulates skeletal muscle growth (McPherron et al., 1997; Szabo et al., 1998). Mstn is mainly synthesized in skeletal muscle as a 376-amino acid propeptide. The active form of Mstn (15 kDa) is expressed at varying levels in many different muscles throughout the body. It is detected very early in the myotome of developing mice (McPherron et al., 1997) and regulates embryonic muscle differentiation (Manceau et al., 2008). The expression levels of Mstn vary, depending on the muscle fiber type or muscle group (Carlson et al., 1999; Sakuma et al., 2000; Wehling et al., 2000). The soleus muscle of Mstn knockout mice displays a larger proportion of fast type II fibers and a reduced proportion of slow type I fibers

(Girgenrath et al., 2005). In Mstn null cattle in a cell culture study, the expression of the fast myosin heavy chains (MyHCs) is also high in vitro (Hayashi et al., 2008). The masseter muscle (MM) exhibits a slower maturation rate than do other muscles at the same embryonic stage in a process that is dependent on the mRNA expression of the MyoD family of genes (Yamane et al., 2000).

The MM more frequently contains type IIX/IIB hybrid fibers than do other skeletal muscles, and its unique composition of muscle fiber types enables it to adapt to tissue-specific functional requirements (Kanbara et al., 1997). The expression pattern of myosin isoforms in this muscle appears later than in other skeletal muscle types, with embryonic-like changes occurring in postnatal MM fibers (Soussi-Yanicostas et al., 1990). There are two major types of muscle fiber, which differ in their myosin heavy chain (MyHC) isoform expression and enzymatic capacities (Pette and Staron, 1990). Type I fibers are red in appearance and have slow-twitch characteristics. They exhibit a high oxidative capacity, utilizing mostly oxidative phosphorylation, and their cytosol is rich in mitochondria (Barnard et al., 1971; Peter et al., 1972). Type II fibers are subdivided into types IIA, IIB and IID/X and display fast-twitch properties. They have a lower oxidative capacity, with fewer mitochondria, and depend on glycolytic metabolism to generate ATP. The rectus femoris muscle (RFM) is a fast-twitch hindlimb muscle consisting of 55% type I and 45% type II muscle fibers (Scholz et al., 2014). The expression of different MyHC isoforms in the MM has been reported to change during developmental stages due to suckling and mastication (Gojo et al., 2002; Widmer et al., 2007). The MM has a different embryonic origin than the RFM, and MM growth is distinct from that of other skeletal muscles. Usami et al. (2003) suggested that the MM differentiation rate is altered and that MyHC IIa expression increases between the pre- and post-natal stages (between E14 and day 5). The composition of muscle fiber in murine masseter is changed at weaning during the transition from suckling to mastication.

The skeletal muscle is a thyroid hormone target, and the MyHC genes are thyroid-activated. The genomic actions of the thyroid hormone are mediated by the thyroid hormone receptor (TR), which is encoded by two genes (expressing the TR-α1/2 and TR-β1/2 isoforms). During development, the transition to each adult MyHC (type I, IIa, IIb and IIx) is mediated by TRα (Yu et al., 2000). The transition from neonatal to adult fast myosin is orchestrated by thyroid hormones acting directly on fast muscle cells in developing euthyroid, hypothyroid and hyperthyroid rats (Gambke et al., 1983). TR-α1 affects MyHC isoform expression during fetal myogenesis and determines the phenotype and function of cardiac and skeletal muscles during development (White et al., 2001; Pircher et al., 2005).

Mstn expression increases in hypothyroid rats, suggesting a possible role for this factor in the pathogenesis of muscle loss that may occur during hypothyroidism (Carneiro et al., 2008). Mstn was strongly downregulated in extraocular muscles isolated from T3-treated animals (Postler et al., 2009). Myostatin also plays a role in muscle metabolic processes regulated by the thyroid hormone (Yi et al., 2009).Therefore, the expression levels of Mstn may be related to those of MyHC or TRα. However, the relationship among Mstn, TRα and MyHC in early postnatal development is not well-understood. Therefore, we examined the expression patterns of Mstn, TRα and MyHCs (slow, embryonic IIa, IIb, and IIx) in the MM and RFM.

Materials and methods

Animals

All laboratory animals were procured from the Nippon Medical Science Animal Resource Laboratory and were bred at the Animal Testing Center of the Dept. of Dentistry, Nippon Dental University. Male mice (CLER JAPN, INC.; Tokyo, Japan) were maintained on a solid pellet diet (MF; Oriental Yeast Inc., Tokyo, Japan). Mice were used at early postnatal days: 0, 2, 4, 6, 8 and 10. The animals were sacrificed by pentobarbital over-dose, and the right MM and RFM were subsequently removed. Fresh samples isolated from the right MM were prepared from six groups. Tissue from each stage (n=4) was used for light microscopy studies and for mRNA and protein analyses by real-time RT-PCR and ELISA, respectively.

Real-time RT-PCR mRNA analyses

Isolation of total RNA

The MM and RFM were immediately removed from each sacrificed mouse by scraping and were stored at -80°C. The muscles were cut into small pieces, and the total RNA was isolated from the samples (0.1 g). Total RNA was extracted using an RNeasy Mini Kit (Qiagen, CA, USA) according to the manufacturer's instructions. Contaminating DNA was removed using RNase-free DNase (DNA-free; Ambion, TX, USA), and the total RNA absorbance at 260 nm was quantified using a spectrophotometer (Biowave S2100; Cambridge, UK). The samples were stored at -80°C until use. Total RNA was converted to cDNA using 0.4 μM random hexamers (N808-0127; Applied Biosystems, CA, USA) in a mixture containing 1 mM of each dNTP, 20 units of RNase inhibitor (2311A; TaKaRa, Tokyo, Japan), 5 units of AMV reverse transcriptase XL (2620A; TaKaRa), 25 mM Tris-HCl (pH 8.3), 50 mM KCl, 2 mM DTT, and 5 mM $MgCl_2$. The following thermal PCR cycling conditions were used: 30°C for 10 min, 42°C for 30 min, 90°C for 5 min, and 5°C for 5 min.

Quantitative real-time RT-PCR

Quantitative real-time RT-PCR was performed using the Applied Biosystems 7300 Fast Real-Time PCR

System (Applied Biosystems, CA, USA) according to the manufacturer's instructions. Each amplification mixture (50 μl) contained 100 ng cDNA, 900 nM forward primer, 900 nM reverse primer, 250 nM fluorogenic probe, and 25 μl Universal PCR Master Mix (Applied Biosystems, CA, USA). The PCR cycling parameters were 50°C for 2 min, 95°C for 10 min, 50 cycles at 95°C for 15 s, and 60°C for 1 min. The following sequences were amplified: embryonic MyHC (Myh3; Mm01332476_m1, Applied Biosystems, CA, USA), slow MyHC (Myh6; Mm00440354_m, Applied Biosystems, CA, USA), MyHC IIa (Myh2; Mm00454991_m1, Applied Biosystems, CA, USA), MyHC IIb (Myh4; Mm01332518_m1, Applied Biosystems, CA, USA), MyHC IIx (Myh1; Mm01332500_gh, Applied Biosystems, CA, USA), Mstn (Mm01254559_m1, Applied Biosystems, CA, USA), and TRα (Thra; Mm00617505_m1, Applied Biosystems, CA, USA). TaqMan Rodent GAPDH Control Reagents with VIC Probe were also used (Applied Biosystems, CA, USA). The abundances of the amplified mouse cDNAs were normalized to those of GAPDH (rodent GAPDH primers and probes were obtained from "Assays-On-Demand", Applied Biosystems, CA, USA).

ELISA

For the ELISA experiments, all tissues were homogenized in 10 volumes of tissue extraction buffer composed of 100 mM Tris pH 7.4, 150 mM NaCl, 1 mM EDTA, 1% Triton X-100, 0.5% sodium deoxycholate, and a protease inhibitor cocktail. The homogenates were centrifuged at 5000 rpm for 5 min, and the protein concentration of the supernatant was determined using the Bradford method (Quick Start Bradford Protein Assay Kit 2, Cat No: #50-0202JA; BioRad, CA, USA). Tissue myostatin levels were assayed using a mouse Mstn ELISA kit (E91653 Mu; Cusabio Biotech Co., Ltd, Hubei Province, China) according to the manufacturer's protocol. The kit's detection range is 3.38 - 600 pg/ml. Tissue homogenates were added to wells pre-coated with a Mstn monoclonal antibody. After incubation, a Mstn antibody labeled with biotin and combined with streptavidin-horseradish peroxidase to form an immune complex was added, followed by incubation with a 3,3',5,5'–tetramethylbenzidine buffer. The resulting blue color was changed to yellow upon the addition of a stop solution to the plate. The plate was read on a microplate reader, and the absorbance at a wavelength of 450 nm was measured.

Light microscopy

Paraffin-embedded blocks and sections of MM and RFM for immunohistochemistry were obtained for day 0 to day 10 mice from Genostaff Co., Ltd (Tokyo, Japan). Mouse embryos were fixed with Tissue Fixative (Genostaff Co., Ltd.), embedded in paraffin using Genostaff's proprietary procedures and sectioned at 6 μm. The tissue sections were deparaffinized with xylene and dehydrated through a series of ethanol solutions in PBS. Endogenous peroxidase was blocked with 0.3% H2O2 in methanol for 15 min, followed by incubation with G-Block (Genostaff Co., Ltd) and an Avidin/Biotin Blocking Kit (Vector SP-2001). The sections were incubated with 0.4 μg/ml of a rabbit polyclonal antibody to dystrophin (Abcam ab15277, Cambridge, England) and with a myostatin rabbit polyclonal antibody (Abcam ab98337) at 4°C overnight. The rabbit immunoglobulin fraction (Dako X0936) was used as a negative control. After washing with TBS, a biotin-conjugated goat anti-rabbit Ig (Dako, Takasaki, Japan) was added at a 1:600 dilution for 30 min at room temperature, followed by the addition of peroxidase-conjugated streptavidin (Nichirei, Tokyo, Japan) for 5 min. Peroxidase activity was visualized by diaminobenzidine. The sections were counterstained with Mayer's Hematoxylin and Eosin (Muto, Tokyo, Japan), dehydrated and then mounted with Malinol. The stained sections were evaluated by microscopy (DM-2500; Leica Microsystems, Germany).

Statistical analysis

The differences in the quantitative real-time RT-PCR and ELISA data among the groups were assessed using two-way analysis of variance (ANOVA, significance was set as $p<0.05$) followed by Bonferroni's post-hoc test with one categorical independent variable and one continuous variable (the independent variable can consist of a number of groups). The level of significance was set as $p<0.05$. The results are reported as the mean ± SD. We performed multivariate modeling in the quantitative data principal component analysis (PCA) to estimate the interaction between the effects of muscle type (MM verse RFM) and early postnatal stage. Then, we performed a cluster analysis (CA) using the average linkage between groups (hierarchical cluster analysis algorithms) based on the significant components of the PCA analysis that was performed on individuals (Cassar-Malek et al., 2007). We calculated the Pearson correlation coefficient for mRNA abundance. The statistical analyses were performed using the IBM SPSS Statistics Base, version 22.

Ethics

All procedures involving mice were reviewed and approved by the Nippon Medical School Animal Resource Laboratory Committee of the Nippon Dental University (No. 09-04).

Results

MyHC mRNA expression in mouse MM and RFM

The mRNA abundance of MyHCs (embryonic, slow, IIa, IIb, and IIx) in the MM and RFM of 0 day to 10 day

mice are shown in Fig. 1. The embryonic MyHC mRNA expression pattern was similar in the two muscles, with abundance rapidly decreasing after birth (Fig. 1a, $p<0.001$). However, significant differences were detected in the other MyHC mRNA abundances between the MM and the RFM (Fig. 1). The slow MyHC mRNA abundance of the MM increased until day 6 ($p<0.001$) and then remained stable, whereas in the RFM, it rapidly decreased from day 0 (Fig. 1b). The MyHC IIa mRNA level in the MM (Fig. 1c) increased from day 6 ($p<0.001$), in contrast to the RFM, where it rapidly decreased from day 2 (Fig. 1c). The MyHC IIb mRNA level in the MM increased from birth and remained stable from days 2 to 10 ($p<0.001$), whereas in the RFM, it rapidly decreased from day 0 (Fig. 1d). The MyHC IIx mRNA abundance increased in the MM from days 6 to 10 ($p<0.001$), but in the RFM, the expression was high at day 2 ($p<0.001$) and low from days 4 to 10

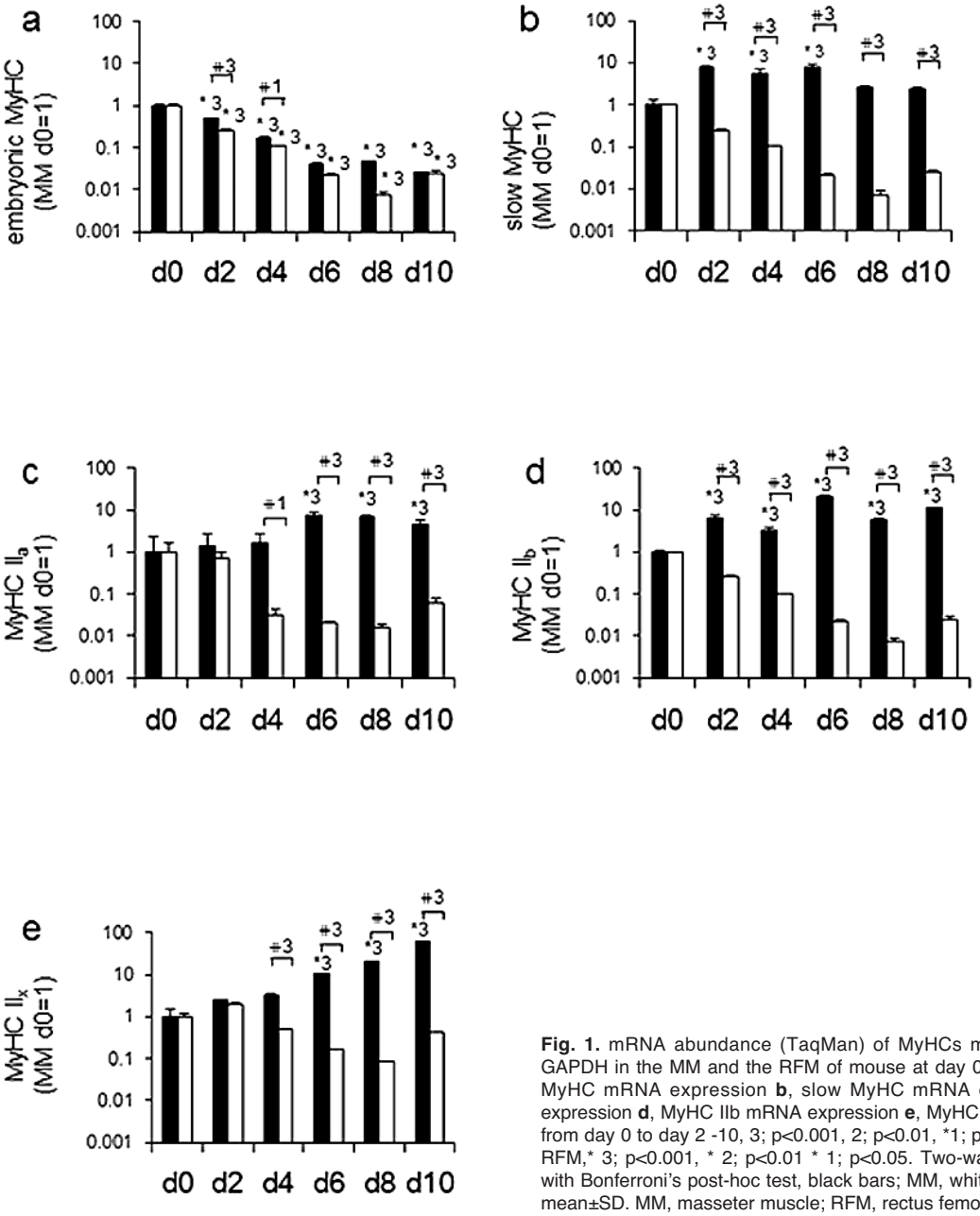

Fig. 1. mRNA abundance (TaqMan) of MyHCs mRNA expression normalized to GAPDH in the MM and the RFM of mouse at day 0, 2, 4, 6, 8 and 10. **a**, embryonic MyHC mRNA expression **b**, slow MyHC mRNA expression **c**, MyHC IIa mRNA expression **d**, MyHC IIb mRNA expression **e**, MyHC IIx mRNA expression. Difference from day 0 to day 2 -10, 3; $p<0.001$, 2; $p<0.01$, *1; $p<0.05$, *; difference from MM and RFM,* 3; $p<0.001$, * 2; $p<0.01$ * 1; $p<0.05$. Two-way analysis of variance (ANOVA) with Bonferroni's post-hoc test, black bars; MM, white bars; RFM, All error bars show mean±SD. MM, masseter muscle; RFM, rectus femoris muscle.

(Fig. 1e).

Expression of Mstn mRNA and protein in mouse MM and RFM

The Mstn mRNA abundance was higher in the MM than in the RFM at days 4-8 ($p<0.001$). In contrast, it was higher in the RFM than in the MM at other times (day 2, $p<0.01$; day 10, $p<0.05$). The Mstn mRNA abundance in the MM gradually increased from day 0 to day 10 and was highest at day 8. In contrast, the Mstn mRNA abundance in the RFM remained constant from day 0 to day 10 and was highest at day 8 (Fig. 2a). The protein levels of Mstn at days 0-10 are shown in Fig. 2b. The MM extract dilutions did not exceed the reference OD obtained from the well containing 50 pg of Mstn. The coefficient of variation was <10%. The Mstn protein was detected in the examined muscles isolated from 0- to 10-day-old mice (Fig. 2b). However, no significant differences were detected between day 0 and the other stages in either the MM or the RFM using Bonferroni's post-hoc test.

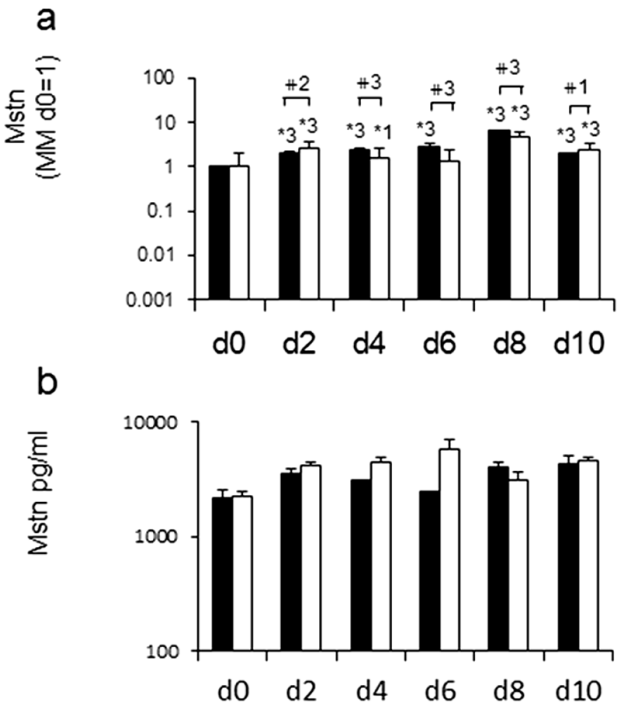

Fig. 2. mRNA of Mstn mRNA expression normalized to GAPDH and the protein of the Mstn in the MM and the RFM of mouse at day 0, 2, 4, 6, 8 and 10. **a.** Mstn mRNA abundance (TaqMan) of each target normalized to GAPDH at days 0, 2, 4, 6, 8 and 10. Difference from day 0 to day 2-10, *3; $p<0.001$, *2; $p<0.01$, *1; $p<0.05$, *; difference from MM and RFM, * 3; $p<0.001$, * 2; $p<0.01$ * 1; $p<0.05$. **b.** Two-way analysis of variance (ANOVA) with Bonferroni's post-hoc test, black bars; MM, white bars; RFM, All error bars show mean ±SD. MM, masseter muscle; RFM, rectus femoris muscle.

Mstn immunohistochemical staining between MM and RFM

Positive staining for the anti-Mstn antibody was localized around the muscle cell nuclei in the MM and RFM at day 0 (Figs. 3a, 4a). Staining was also clearly present in the muscle cells of the MM and RFM cross-sections at day 4 and 10 (Figs. 3e,g,h,i, 4e,i,k,l). In contrast, positive staining for the anti-dystrophin antibody localized around the cell membranes of the muscle fibers (Figs. 3b,f,j, 4b,f,j). Furthermore, the Mstn reaction zone was clearly distinguished from the dystrophin reaction area in the two muscles. Mstn antibody staining was mainly strong in the area linked to the muscle fiber surface beginning at day 0 and day 4 (Figs. 3a,e,c,g,d,h, 4a,e,c,g,d,h).

TRα mRNA expression in the mouse MM and RFM

The TRα mRNA abundance was higher in the MM than in the RFM at days 2, 4, 6, 8 ($p<0.001$) and 10 ($p<0.05$). The mRNA abundance of TRα in the MM gradually increased from day 0, peaked at day 6 ($p<0.001$), and remained stable at days 8 and 10 ($p<0.001$). However, the TRα mRNA abundance in the RFM was high at day 0 and then decreased rapidly until day 10 (Fig. 5).

Principal component analysis (PCA) and cluster analysis

PCA was performed for the MM and RFM at different early postnatal stages and the expression of the following 7 mRNAs: Mstn, TRα, embryonic MyHC, slow MyHC, MyHC IIa, MyHC IIb and MyHC IIx (Fig. 6). The variables were plotted in a two-dimensional space defined by the two axes of component 1 (x axis) and component 2 (y axis) for each muscle (Fig. 6a,b in the MM and RFM, respectively). The two principal components significantly explained 74.5% (component 1, 48.3%; component 2, 26.2%) of the information in the dataset for the MM (Fig. 6a). In the MM, the most important variable explaining component 1 was embryonic MyHC. The first component illustrated the negative correlation between embryonic MyHC and all other variables and the progressive myosin transition with age (contractile differentiation): disappearance of the developmental myosin with increasing age and its replacement by the adult forms. Component 2 was explained mainly by the metabolic (TRα) and contractile properties of the muscle and illustrated the opposition between Mstn and the slow oxidative type (MyHC slow).

The two principal components significantly explained 87.2% (component 1, 73.4%; component 2, 13.8%) of the information in the dataset for the RFM (Fig. 6b). In the RFM, the most important variables explaining component 1 were the transcripts of all MyHC and TRα. The first component illustrated myosin transition with age: disappearance of the developmental

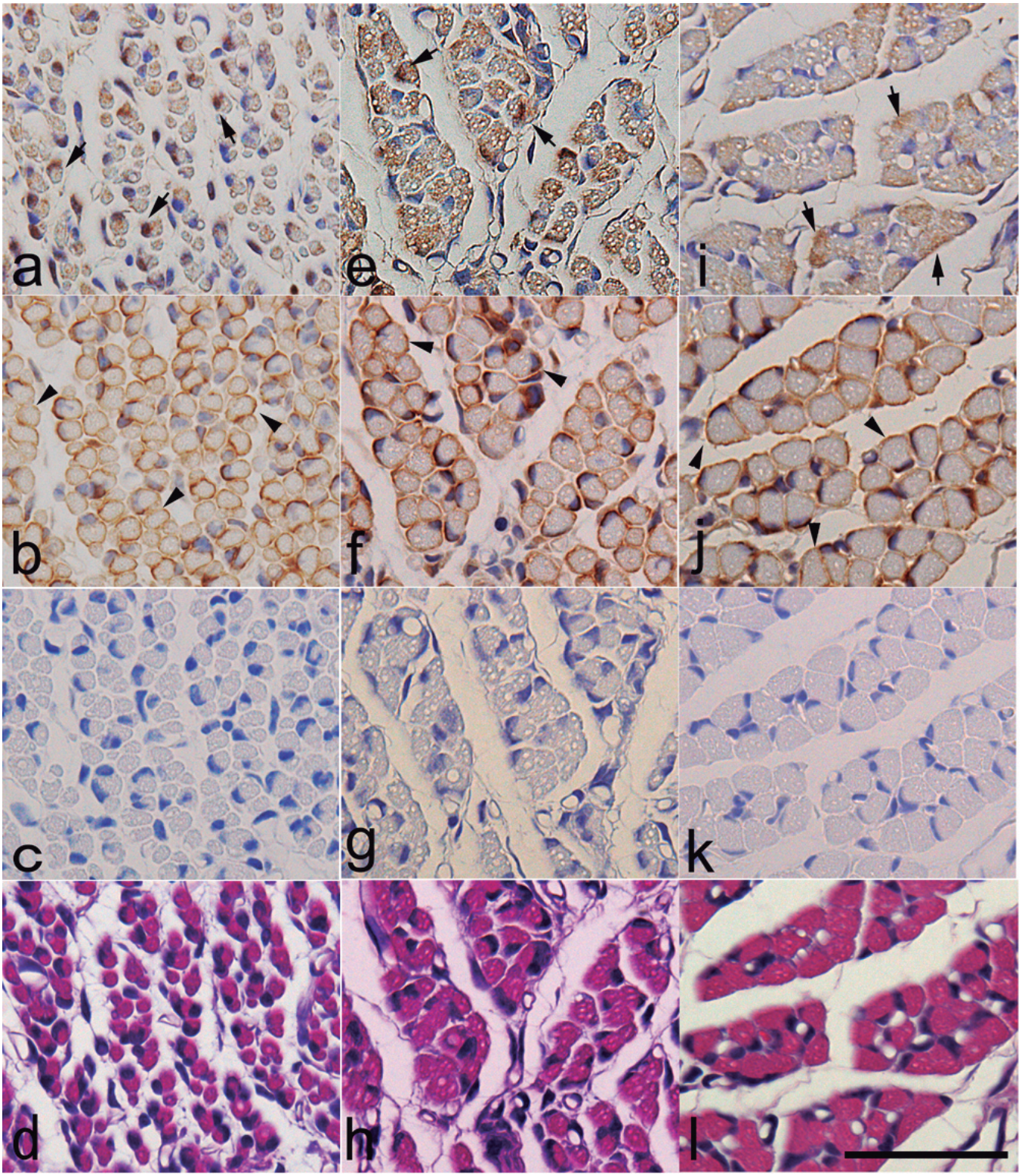

Fig. 3. Immunohistochemical staining for Mstn and dystrophin in the MM isolated at 0-, 4- and 10-day old mice. A positive Mstn signal is indicated by arrows in the muscle fibers in the nuclei. Dystrophin-positive signals around the muscle fibers are indicated by arrowheads. **a.** Mstn staining at day 0. **b.** Dystrophin staining at day 0. **c.** Negative control at day 0. **d.** Hematoxylin and Eosin staining at day 0. **e.** Mstn at day 4. **f.** Dystrophin staining at day 4. **g.** Negative control at day 4. **h.** Hematoxylin and Eosin staining at day 4. **i.** Mstn staining at day 10. **j.** Dystrophin staining at day 10. **k.** Negative control at day 10. **l.** Hematoxylin and Eosin staining at day 10. Bar: 50 μm.

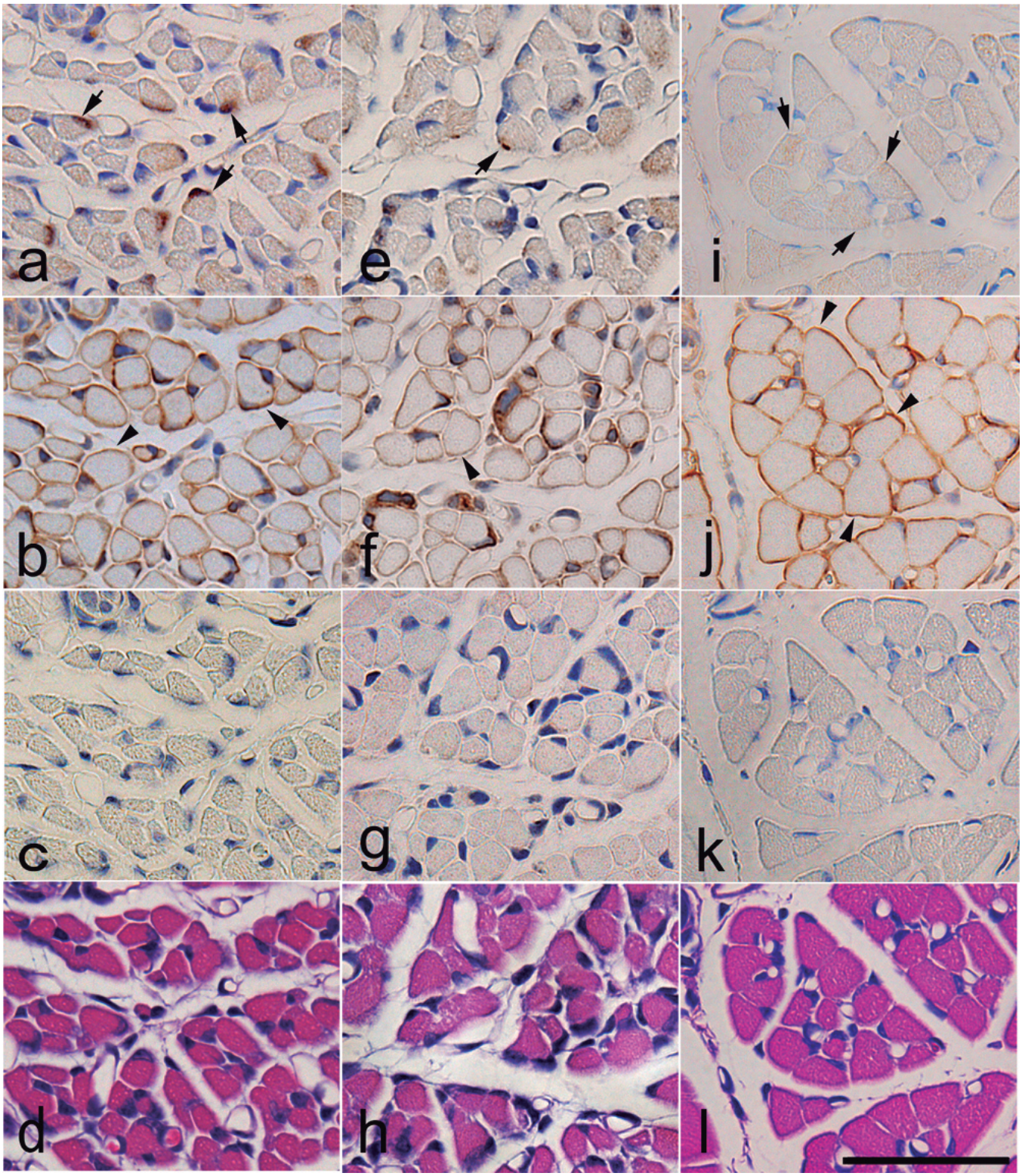

Fig. 4. Immunohistochemical staining for Mstn and Dystrophin in the RFM isolated in 0-, 4-and 10-day old mice. A positive Mstn signal is indicated by arrows in the muscle fibers in the nuclei. Dystrophin-positive signals around the muscle fibers are indicated by arrowheads **a.** Mstn staining at day 0. **b.** Dystrophin staining at day 0. **c.** Negative control at day 0. **d.** Hematoxylin and Eosin staining at day 0. **e.** Mstn at day 4. **f.** Dystrophin staining at day 4. **g.** Negative control at day 4. **h.** Hematoxylin and Eosin staining at day 4. **i.** Mstn staining at day 10. **j.** Dystrophin staining at day 10. **k.** Negative control at day 10. **l.** Hematoxylin and Eosin staining at day 10. Bar: 50 μm.

myosin with increasing age and its replacement by the adult forms. Component 2 was explained mainly by the metabolic (TRα) and contractile properties of the muscle and illustrated the opposition between Mstn and fast glycolytic type (MyHC IIx).

In addition, we performed clustering analysis using a hierarchical classification model with these two components demonstrating that optimal grouping was obtained with three clusters (Fig. 7a,b). In the MM, the characterization of the three clusters was separated by aging. Cluster 1 included samples from days 0 to 4, whereas cluster 2 was exclusively composed of day 6 samples. Cluster 3 was composed of samples from days 8 to 10 (Fig. 7a). In the MM, cluster 3, corresponding to the oldest stages (days 8 and 10), was characterized by its high Mstn and MyHC IIa expressions and low embryonic MyHC expression. Cluster 2 was characterized by its intermediate Mstn expression and

Table 1. Muscle type, day and mRNA expression from MM in the clusters.

	cluster1	cluster2	cluster3	P value
Mstn	1.00±0.06 #	2.31±0.42 #*	6.38±0.21 *	<0.001
TRα	1.00±0.16	2.20±0.58 #*	0.88±0.26	<0.001
embryonic MyHC	1.00±0.08 #	0.17±0.019	0.046±0.00 *	<0.001
slow MyHC	1.00±0.27	5.87±2.54	2.53±0.35	<0.01
MyHC IIa	1.00±1.27 #	3.87±2.85	6.95±0.29 *	<0.05
MyHC IIb	0.99±0.108	10.27±6.67	5.84±0.39	0.06
MyHC IIx	1.00±0.53	19.37±25.5	20.20±0.22	0.425

Table 2. Muscle type, day and mRNA expression from RFM in the clusters.

	cluster1	cluster2	cluster3	P value
Mstn	1.00±0.14 #	1.97±0.055 #*	4.81±0.21 *	<0.001
TRα	0.91±0.021 #	0.06±0.07 *	0.007±0.00 *	<0.001
embryonic MyHC	1.00±0.028 #	0.10±0.01 *	0.007±0.001 *	<0.001
slow MyHC	1.00±0.028 #	0.10±0.01 *	0.007±0.001 *	<0.001
MyHC IIa	1.00±0.71 #	0.20±0.33 *	0.015±0.004 *	<0.05
MyHC IIb	1.00±0.03 #	0.10±0.09 *	0.007±0.001 *	<0.001
MyHC IIx	0.99±0.14	0.77±0.76	0.082±0.003	0.215

Results are expressed as the mean ±SD. *p<0.05 vs. cluster 1 and #p<0.05 vs. cluster 3 using a post hoc Bonferroni test.

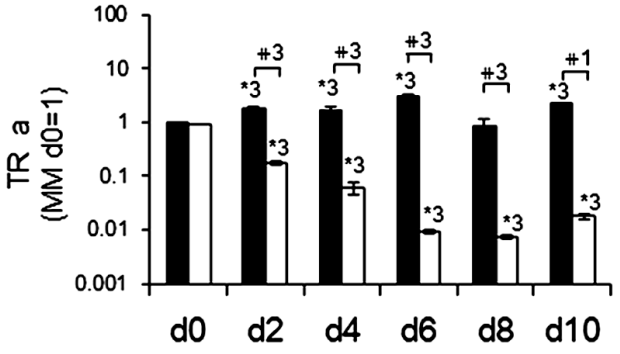

Fig. 5. TRα mRNA abundance (TaqMan) of each target normalized to GAPDH in the MM and the RFM at days 0, 2, 4, 6, and 8. Difference from day 0 to day 2-10, 3; p<0.001,*2; p <0.01, *1; p <0.05, *; difference from MM and RFM, -* 3; p<0.001, 2; p <0.01 1; p <0.05. Two-way analysis of variance (ANOVA) with Bonferroni's post-hoc test, black bars; MM, white bars; RFM, All error bars show the mean ±SD. MM, masseter muscle; RFM, rectus femoris muscle.

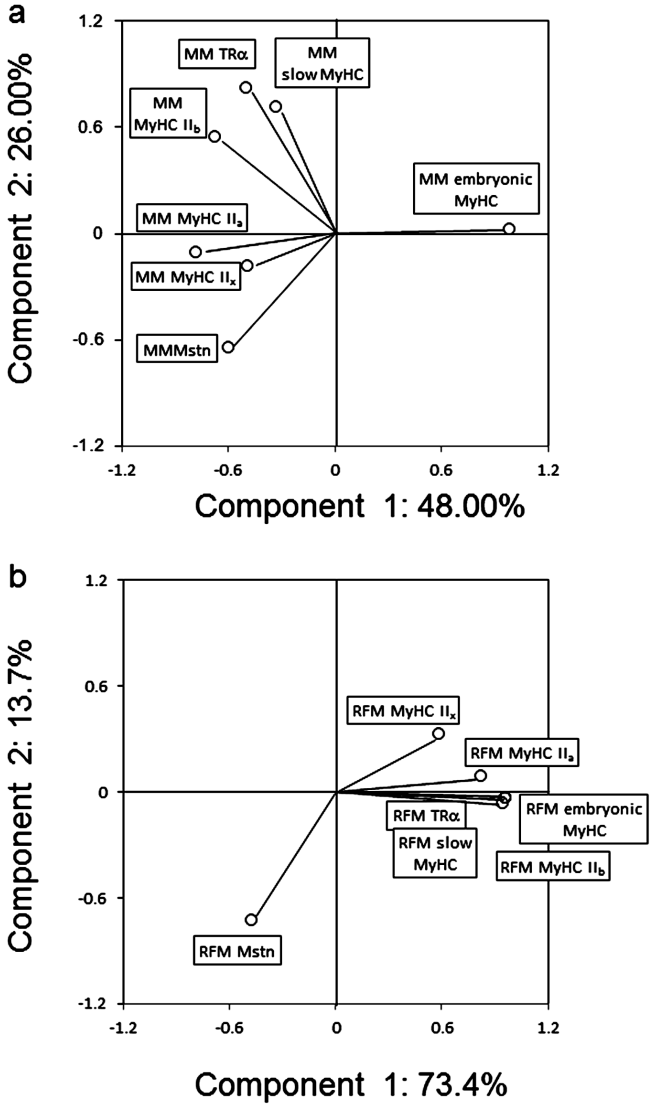

Fig. 6. Gene expression levels in MM and RFM using TaqMan Gene Expression Assays by principal component analysis (PCA). The original variables are indicated by component 1 (x-axis) and component 2 (y-axis). a, MM, masseter muscle (axis component 1 and component 2: 74.0%). b, RFM, rectus femoris muscle (axis component 1 and component 2: 87.1%).

high TRα expression (Tables 1, 2). In the RFM, the characterization of the three clusters was also separated by aging. Cluster 1 included aging time-points at day 0, whereas cluster 2 contained day 2 samples. Cluster 3 grouped samples from days 4 to 10 in the RFM (Fig. 7b). In RFM, cluster 3 (days 4-10) was mainly characterized by high Mstn expression and very low MyHC expression, and cluster 2 was intermediate (Tables 1, 2).

The expression of the Mstn mRNA in the MM and RFM was significantly higher in clusters 2 and 3 compared with cluster 1 (Tables 1, 2, $p<0.05$).The expressions of the RFM MyHC (embryonic MyHC, slow MyHC, MyHC IIa and MyHC IIb) were significantly lower in clusters 2 and 3 compared with cluster 1 ($p<0.05$) (Table 2). In the MM, the mRNA level of embryonic MyHC was significantly lower in cluster 3 compared with cluster 1 ($p<0.05$) and that of MyHC IIa was significantly enhanced in cluster 3 compared with cluster 1 ($p<0.05$) (Table 1). We observed a positive correlation between MM Mstn and MM MyHC (IIa and IIx) and a negative correlation between MM Mstn and MM embryonic MyHC (Fig. 7a). In contrast, a negative correlation was observed between RFM Mstn and RFM MyHCs (embryonic, slow and IIb) and TRα (Fig. 7b).

The following correlations among the mRNA expression abundance of MyHCs, Mstn and TRα in the MM and RFM since day 0 are shown in Table 3: positive correlation between MM Mstn and MM MyHC IIa ($r>0.627$; $p<0.01$); negative correlation between MM Mstn and MM embryonic MyHC ($r>0.554$; $P<0.01$); positive correlation between MM TRα and MyHC IIb ($r>0.867$; $p<0.01$) and MM slow MyHC ($r>0.605$; $p<0.01$); negative correlation between MM TRα and MM embryonic MyHC ($r>0.469$; $p<0.05$); negative correlation between Mstn and all other variables, except for MyHC IIa and MyHC IIx in the RFM ($p<0.05$); and a negative correlation between TRα and MyHCs, except for MyHC IIx($p<0.05$).

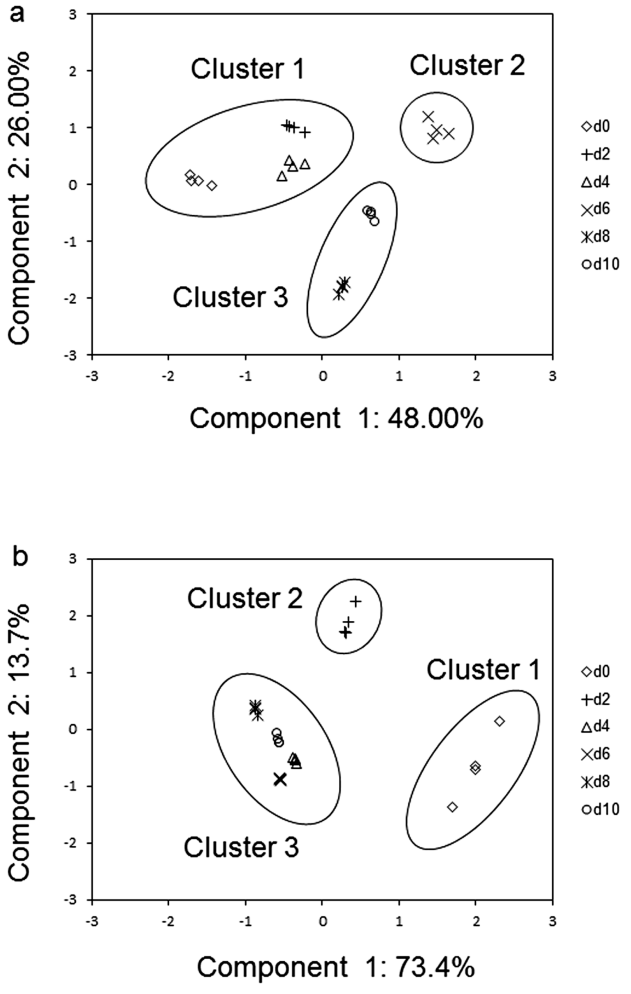

Fig. 7. Factor map obtained in all individual samples from MM and RFM. Reduced dimension of the gene expression levels by PCA were characterized by cluster analysis (CA). The original variables are indicated by component 1 (x-axis) and component 2 (y-axis). Each symbol belongs to a specific cluster. a, MM, masseter muscle. b, RFM, rectus femoris muscle. *, day 0; +, day 2; Δ, day 4; ×, day 6; ✳ day 8; ○ day 10.

Discussion

Mstn and MyHCs and their relationships in the MM and RFM

MM and RFM develop from elements of different origin (branchial arch verse somite) and function (non-locomotor vs. locomotor muscle) (Sperber, 2001). MM originates from the head somitomeres and the first branchial arch during cranio-facial muscle formation; in contrast, RFM originates from the somites, specifically from the myotome layer of the somite (Noden and Francis-West, 2006). RFM is a locomotor limb muscle involved in movement (Allen and Leinwand, 2001); in contrast, MM is a masticatory muscle and its activity changes with changing feeding patterns during postnatal development, especially at weaning (Gojo et al., 2002, Usami et al., 2003; Widmer et al., 2007). Muscles of mastication, including MM, are non-locomotor and differ from limb muscles in some metabolic and contractile properties (Rowlerson et al., 1981, 1983; d'Albis et al., 1986; Mabuchi et al. 1984; Soussi-Yanicostas et al. 1990; Monemi et al. 1999). The differences detected in the expression patterns of MyHC and Mstn in RFM and MM may be explained by differences in developmental origin and activity. Firstly, the early development of head and limb muscles is controlled by different pathways (Tzahor, 2009). In our result, PCA was performed for the MM and RFM at different early postnatal stages and the expression of the following 7 mRNAs: Mstn, TRα, embryonic MyHC, slow MyHC, MyHC IIa, MyHC IIb and MyHC IIx (Fig.

6). In the head, specifically in the branchial derived muscles, myogenesis depends primarily on myf5/mrf4 and MyoD (Yamane et al., 2000). The upstream regulators are different from those of the body and limb; pax3 is not expressed and pax7 is activated later (Bismuth and Relaix, 2010)

We have detected muscle-specific relationships between the studied variables as illustrated by the different clustering of the animals in the two muscles. These relationships are described by a negative correlation between Mstn transcripts and embryonic, IIb, and slow MyHCs in the RFM and MyHC in the MM and a positive correlation with MyHC IIa in the MM. Mstn expression has been positively associated with MyHC IIb expression in several hindlimb muscles of normal mice (Carlson et al., 1999), and some authors have suggested that the MyHC IIb phenotype could be a consequence of the impact of myostatin on the regulators of muscle phenotype (Hennebry et al., 2009). Conversely, in our study, Mstn expression was inversely correlated with MyHC IIb in the RFM, but no correlation was detected in the MM at the early postnatal stage. This discrepancy was explained by Girgenrath et al. (2005) who found that inhibition of Mstn in adult skeletal muscle does not cause a transformation to a faster and glycolytic phenotype and also suggests that Mstn has a critical role in regulating the formation, proliferation, or differentiation of postnatal fibers.

Different Mstn and MyHC expressions between MM and RFM are classified by the group of postnatal days in the cluster analysis. In our study, each cluster of expression contained different factors from among the MM and RFM by age: cluster 1 (MM (days 0, 2, 4) vs RFM (day 0)), cluster 2 (MM (day 6) vs RFM (day 2), cluster 3 (MM (days 8, 10) vs RFM (days 4, 6, 8, 10)) (see Fig. 7). Therefore, the three clusters defined by aging for the MM and the RFM remained independent during development. The ELISA data demonstrated that the Mstn protein expression levels did not vary significantly each day despite accurate quantitative measurements of differences in the mRNA transcripts. Mstn is modulated, stored and secreted in the extracellular matrix (ECM) during skeletal muscle development (Miura et al., 2010). Mstn trapped in the extracellular matrix can affect secretion and account for the observed expression differences. In general, Mstn is secreted by muscle cells, which release the propeptide from the mature region of Mstn. The mature region binds the type II activin receptor on the cell membrane surface. Finally, it facilitates Smad2/3 phosphorylation and translocation into the nucleus, where it initiates gene transcription (Lee and McPherron, 2001; Langley et al., 2002; Shi and Massague, 2003). Our immunohistochemical analyses showed that anti-Mstn antibody staining was localized to the cell membrane surface in the MM. Positive Mstn staining was observed around the nuclei and muscle fibers in the MM at day 0, and strong staining was then detected in the linked zone of muscle fibers in addition to the nuclear zone of the muscle cells from day 4. Mstn localization varied from days 0 to 4, at which time it spread out and was localized around the muscle cells. Therefore, Mstn may be stored and

Table 3. Correlation coefficients between the abundance of mRNA from MM and RFM.

		MM							RFM						
	gene	M stn	TRα	embryonic MyHC	slow MyHC	MyHC IIa	MyHC IIb	MyHC IIx	Mstn	TRα	embryonic MyHC	slow MyHC	MyHC IIa	MyHC IIb	MyHC IIx
MM	Mstn	1.000													
	TRα	-0.279	1.000												
	embryonic MyHC	-0.554**	-0.469*	1.000											
	slow MyHC	-0.044	0.605**	-0.282	1.000										
	MyHC IIa	0.627**	0.388	-0.698**	0.084	1.000									
	MyHC IIb	0.099	0.867**	-0.604**	0.483*	0.724**	1.000								
	MyHC IIx	0.090	0.207	-0.520*	-0.368	0.368	0.326	1.000							
RFM	Mstn	0.870**	-0.416*	-0.440*	-0.160	0.403*	-0.095	0.279	1.000						
	TRα	-0.523*	-0.473*	0.959**	-0.463*	-0.566**	-0.553**	-0.404*	-0.468*	1.000					
	embryonic MyHC	-0.545**	-0.467*	0.974**	-0.423*	-0.611**	-0.569**	-0.435*	-0.481*	0.997**	1.000				
	slow MyHC	-0.545**	-0.467*	0.974**	-0.423*	-0.611**	-0.569**	-0.435*	-0.481*	0.997**	1.000**	1.000			
	MyHC IIa	-0.456*	-0.344	0.843**	-0.124	-0.633**	-0.430*	-0.382	-0.280	0.744**	0.762**	0.762**	1.000		
	MyHC IIb	-0.545**	-0.467*	0.974**	-0.423*	-0.611**	-0.569**	-0.435*	-0.481*	0.997**	1.000**	1.000**	0.762**	1.000	
	MyHC IIx	-0.495*	-0.137	0.606**	0.310	-0.704**	-0.370	-0.381	-0.191	0.372	0.425*	0.425*	0.671**	0.425*	1.000

**: significant at P<0.01; *: significant at P<0.05

secreted into the ECM during muscle development, as previously reported (Anderson et al., 2008; Hosaka et al., 2009; Yasaka et al., 2013).

TRα and its relationships to MyHC in the MM and RFM

Thyroid hormone (TH) is involved in vertebrate development and growth. In muscle, TH specifically regulates MyHCs in different skeletal muscles (Gambke et al., 1983; Pircher et al., 2005) and tongue muscles (Sato et al., 2006). d'Albis et al. (1990) reported that TH drives the MyHC transition of rat MM after birth. Izumo et al. (1986) reported that TH regulated the expression of the fast IIB MyHC in the MM of rats. TH plays a role in the switching MyHC phenotype in pig through changes in myogenic regulatory factor levels (Dauncey and Gilmour, 1996; Dauncey and Harrison, 1996). The effect of TH is mediated by DNA binding receptors acting as transcription factors called TRα and TRβ. TH binds to TRα and directly activates transcription of the myosin heavy chain genes (Izumo and Mahdavi, 1988) through thyroid-responsive elements in the promoter of these TH-responsive genes. Allen and Leinwand (2001) suggested that the specialized shifts in the MyHC isoform in skeletal muscle are related to both thyroid/hormonal status and muscle activity during postnatal development. TRα expression is important for the induction and differentiation of muscles (pig, White et al., 2001; Chicken, Svensson Holm et al., 2014). Our data agree with these reports, as shown by a positive correlation between TRα and IIb and slow MyHC expressions in the MM. A positive correlation between TRα and MyHC transcript abundance, except for the IIx isoform, was also detected in the RFM. Therefore, the liganded-TRα regulates the contractile properties of muscle by driving MyHC isoform expression in each muscle during the early postnatal stage. Our principal component analysis indicated that in the RFM, the expression of all MyHCs (IIa, IIb, slow, embryonic) are significantly positively correlated with that of TRα. MyHC IIx is negatively correlated with TRα In contrast, MyHCs (IIb, slow) expression is correlated with that of TRα in the MM. This illustrated a muscle-specific effect of T3 mediated by TRα for embryonic MyHC because the direction of the correlation was different between muscles. The different TRα and MyHC expressions between MM and RFM are regulated by the time course by cluster analysis. TRα may thus affect and regulate the contractile properties of muscle by driving MyHC isoform expression. TRα drives MyHCs to and then diminishes embryonic MyHC with age in the MM. Both the increase in the T3 level and the up-regulation of TR in the skeletal muscle may have a direct role in the regulation for switching phenotype MyHCs after birth, in contrast to that of the MM. White et al. (2001) only indicated that the level of mRNA of TRα is high at 20 embryonic gestation (E20), and gradually decreased from E20 to adults in pig skeletal muscles. However, there are no data on TRα expression in MM from the embryo to early postnatal stages. TRα and MyHCs mRNA expressions in the MM patterns are also different than that of the RFM from day 0 to day 10 in our results. In rat skeletal muscle, the mRNA of TRα is clearly different from day 10 to day 20 compared to that of adults (3-4 months old) between fast-twitch and slow-twitch muscles (Schuler and Pette, 1998). A different expression pattern of the MyHC isoform of the MM suggested that the feeding pattern is changed from suckling to mastication 2-3 weeks after birth (Gojo et al., 2002). Therefore, despite the different abundance between TRα and MyHCs in the RFM, TRα exerted a limited effect on MyHCs compared to that of the MM at the early postnatal stages, as shown by our principal component analysis.

Relationships between Mstn and THα

There are little data relating Mstn to TR. Thyroid hormone receptor regulates Mstn levels in muscles (Ortiz et al., 1995). Hypothyroidism is associated with increased myostatin expression in rats (Carneiro et al., 2008; Yi et al., 2009), which may be linked by the presence of several putative thyroid hormone response elements in the myostatin promoter region. Mstn and thyroid hormone-associated protein 1 are related to miR-2008, which is a family of miRNAs in adult mouse heart physiology (Callis et al., 2009). The miR-208 factor functions in cardiomyocytes regulating MyHCs during development (Malizia and Wang, 2011) and stress and hormonal signaling (van Rooij et al., 2007). The Mstn and thyroid hormone in the MM may also be regulated by stress from suckling to mastication with the development jaw muscles.

Our principal component analysis results indicated that in the RFM, Mstn expression is negatively correlated with that of TRα. This suggests that TH may negatively regulate myostatin in a muscle destined to contain IIX>IIA or IIB fibers. In contrast, Mstn expression is not correlated with that of the MM, especially in MyHC IIx. Therefore, Mstn likely exerted a limited effect on TRα compared to that detected in the MM at early postnatal stages. Therefore, the early postnatal stages of development have a limited effect on Mstn expression in the RFM, despite having a similar expression pattern to Mstn between the RFM and MM. TRα is involved in the temporal expression of MyHCs in the MM, despite having a different expression pattern between the RFM and MM in our study. The MyHCs patterns of MM are affected by the functional properties because suckling transitions to weaning within 10 days postnatal. In contrast, the MyHcs patterns of RFM may be slightly induced by Mstn and TRa within 10 days postnatal.

In our immunohistochemical observation and based on the transcription levels of myogenic markers (Mstn, embryonic MyHC, slow fiber MyHC, MyHC IIb, MyHC IIa, and IIx) and muscle metabolic marker (TRα) analysis, TRα potentially influences MyHCs expression

in both MM and RFM. Mstn may affect the MM MyHC expression related to muscle development compared to the RFM at early postnatal developmental stages. Moreover, more information is needed about a specific functional event related to Mstn, TRα and MyHCs expressions after birth changing from suckling to mastication with the development of jaw muscles.

Conflict of Interest: None

References

Allen D.L and Leinwand L.A. (2001). Postnatal myosin heavy chain Isoform expression in normal mice and mice null for IIb or IId myosin heavy chains. Dev. Biol. 229, 383-395.

Anderson S.B., Goldberg A.L. Whitman M. (2008). Identification of a novel pool of extracellular pro-myostatin in skeletal muscle. J. Biol.Chem. 283, 7027-7035.

Barnard R.J., Edgerton V.R., Furukawa T. and Peter J.B. (1971). Histochemical, biochemical, and contractile properties of red, white, and intermediate fibers. Am. J. Physiol. 10, 410-414.

Bismuth K. and Relaix F. (2010). Genetic regulation of skeletal muscle development. Exp. Cell Res. 316, 3081-3086.

Callis T.E., Pandya K., Seok H.Y., Tang R.H., Tatsuguchi M., Huang Z.P., Chen J.F., Deng Z., Gunn B., Shumate J., Willis M.S., Selzman C.H. and Wang D.Z. (2009). MicroRNA-208a is a regulator of cardiac hypertrophy and conduction in mice. J. Clin. Invest. 119, 2772-2786.

Carlson C.J., Booth F.W. and Gordon S. E. (1999). Skeletal muscle myostatin mRNA expression is fiber-type specific and increases during hindlimb unloading. Am. J. Physiol. 277, R601-R606.

Carneiro I., Castro-Piedras I., Muñoz A., Labandeira-García J.L., Devesa J. and Arce V.M. (2008). Hypothyroidism is associated with increased myostatin expression in rats. J. Endocrinol. Invest. .31, 773-778.

Cassar-Malek B., Picard S. and Kahl J.F. (2007). Hocquette Relationships between thyroid status, tissue oxidative metabolism, and muscle differentiation in bovine fetuses. Domest. Anim. Endocrinol. 33, 91-106.

d'Albis A., Janmot C. and Bechet J.J. (1986). Comparison of myosins from the masseter muscle of adult rat, mouse and guinea-pig. Persistence of neonatal-type isoforms in the murine muscle. Eur. J Biochem. 156 ,291-296.

d'Albis A., Chanoine C., Janmot C., Mira J.C. and Couteaux R. (1990). Muscle-specific response to thyroid hormone of myosin isoform transitions during rat postnatal development. Eur. J. Biochem. 193, 155-161.

Dauncey M.J. and Gilmour R.S. (1996). Regulatory factors in the control of muscle development. Proc. Nutr. Soc. 55, 543-559.

Dauncey M.J. and Harrison A.P. (1996). Developmental regulation of cation pumps in skeletal and cardiac muscle. Acta Physiol. Scand. 156, 313-323.

Gambke B., Lyons G.E., Haselgrove J., Kelly A.M. and Rubinstein N.A. (1983). Thyroidal and neural control of myosin transitions during development of rat fast and slow muscles. FEBS Lett. 156, 335-339.

Girgenrath S., Song K. and Whittemore L.A. (2005). Loss of myostatin expression alters fiber-type distribution and expression of myosin heavy chain isoforms in slow- and fast-type skeletal muscle. Muscle Nerve 31, 34-40.

Gojo K., Abe S. and Ide Y. (2002). Characteristics of myofibres in the masseter muscle of mice during postnatal growth period. Anat. Histol. Embryol. 31, 105-112.

Hayashi S., Miyake M., Watanabe K., Aso H., Hayashi S. and Ohara S. (2008). Myostatin preferentially down-regulates the expression of fast 2x myosin heavy chain in cattle. Proc. Jpn. Acad. Ser. B Phys. Biol. Sci. 84, 354-362.

Hennebry A., Berry C., Siriett V., O'Callaghan P., Chau L., Watson T., Sharma M, and Kambadur R. (2009). Myostatin regulates fiber-type composition of skeletal muscle by regulating MEF2 and MyoD gene expression. Am. J. Physiol. Cell. Physiol. 296, C525-C534.

Hosaka Y.Z., Ishibashi M., Wakamatsu J., Uehara M. and Nishimura T. (2009). Myostatin regulates proliferation and extracellular matrix mRNA expression in NIH3T3 fibroblasts. Biomed. Res. 33, 355-361.

Izumo S. and Mahdavi V. (1988). Thyroid hormone receptor alpha isoforms generated by alternative splicing differentially activate myosin HC gene transcription. Nature 334, 539-542.

Izumo S., Nadal-Ginard B. and Mahdavi V. (1986). All members of the MHC multigene family respond to thyroid hormone in a highly tissue-specific manner. Science 231, 597-600.

Kanbara K., Sakai A., Watanabe M., Furuya E. and Shimada M. (1997). Distribution of fiber types determined by in situ hybridization of myosin heavy chain mRNA and enzyme histochemistry in rat skeletal muscles. Cell Mol. Biol. (Noisy-le-grand). 43, 319-327.

Langley B., Thomas M., Bishop A., Sharma M., Gilmour S. and Kambadur R. (2002). Myostatin inhibits myoblast differentiation by downregulating MyoD expression. J. Biol. Chem. 277, 49831-49840.

Lee S.J. and McPherron A.C. (2001). Regulation of myostatin activity and muscle growth. Proc. Natl. Acad. Sci. USA 98, 9306-9311.

Mabuchi K., Pinter K., Mabuchi Y., Sreter F. and Gergely J. (1984). Characterization of rabbit masseter muscle fibers. Muscle Nerve 7, 431-438.

Malizia A.P. and Wang D.Z. (2011). MicroRNAs in cardiomyocyte development. Systems Biol. Med. 3, 183-190.

Manceau M., Gros J., Savage K., Thome V., McPherron A., Paterson B. and Marcelle C. (2008). Myostatin promotes the terminal differentiation of embryonic muscle progenitors. Genes Dev. 22, 668-681.

McPherron A.C., Lawler A.M. and Lee S.J. (1997). Regulation of skeletal muscle mass in mice by a new TGF-beta superfamily member. Nature 387, 83-90.

Miura T., Kishioka Y., Wakamatsu J., Hattori A. and Nishimura T. (2010). Interaction between myostatin and extracellular matrix components. Anim. Sci. J. 81, 102-107.

Monemi M., Eriksson P.O., Kadi F., Butler-Browne G.S. and Thornell L.E. (1999). Opposite changes in myosin heavy chain composition of human masseter and biceps brachii muscles during aging. J. Muscle Res. Cell Motil. 20, 351-361.

Noden D.M. and Francis-West P. (2006). The differentiation and morphogenesis of craniofacial muscles. Dev. Dyn. 235.1194-1218.

Ortiz M.A., Piedrafita F.J., Pfahl M. and Maki R. (1995). TOR: a new orphan receptor expressed in the thymus that can modulate retinoid and thyroid hormone signals. Mol. Endocrinol. 9, 1679-1691.

Peter J.B., Barnard R.J., Edgerton V.R., Gillespie C.A. and Stempel K.E. (1972). Metabolic profiles of three fiber types of skeletal muscle in guinea pigs and rabbits. Biochemistry 10, 2627-2633.

Pette D. and Staron R.S. (1990). Cellular and molecular diversities of

mammalian skeletal muscle fibers. Rev. Physiol. Biochem. Pharmacol. 10, 1-76.

Pircher P., Chomez P., Yu F., Vennstrom B. and Larsson L. (2005). Aberrant expression of myosin isoforms in skeletal muscles from mice lacking the rev-erbAalpha orphan receptor gene. Am. J. Physiol. Regul. Integr. Comp. Physiol. 288: 482-490.

Postler T.S., Budak M.T., Khurana T.S. and Rubinstein N.A. (2009). Influence of hyperthyroid conditions on gene expression in extraocular muscles of rats. Physiol. Genomics 37, 231-238.

Rowlerson A., Pope B., Murray J., Whalen R.G. and Weeds A.G. (1981). A novel myosin present in cat jaw-closing muscles. J. Muscle Res. Cell Motil. 2, 415-428.

Rowlerson A., Mascarello F., Veggetti A. and Carpene E. (1983). The fibre-type composition of the first branchial arch muscles in Carnivora and Primates. J. Muscle Res. Cell Motil. 4, 443-472.

Sakuma K., Watanabe K., Sano M., Uramoto I. and Totsuka T. (2000). Differential adaptation of GDF8/myostatin, FGF6 and leukemia inhibitory factor in overloaded, regenerating and denervated rat muscles. Biochem. Biophy. Acta 1497, 77-88.

Sato I., Miyado M., Miwa Y. and Sunohara M. (2006). Expression of nuclear and mitochondrial thyroid hormone receptors in postnatal rat tongue muscle. Cells Tissues Organs 183,195-205.

Scholz K., Kynast A.M., Couturier A., Mooren F.C., Krüger K., Most E., Eder K. and Ringseis R. (2014). Supplementing healthy rats with a high-niacin dose has no effect on muscle fiber distribution and muscle metabolic phenotype. Eur. J. Nutr. 53, 1229-1236.

Schuler M.J. and Pette D. (1998). Quantification of thyroid hormone receptor isoforms, 9-cis retinoic acid receptor gamma, and nuclear receptor co-repressor by reverse-transcriptase PCR in maturing and adult skeletal muscles of rat. Eur. J. Biochem. 257, 607-14.

Svensson Holm A.C., Lindgren I., Osterman H. and Altimiras J. (2014). Thyroid hormone does not induce maturation of embryonic chicken cardiomyocytes in vitro. Physiol. Rep. 2, e12182.

Shi Y. and Massague J. (2003). Mechanisms of TGF-beta signaling from cell membrane to the nucleus. Cell 113, 685-700.

Soussi-Yanicostas N., Barbet J.P., Laurent-Winter C., Barton P. and Butler-Browne G.S. (1990). Transition of myosin isozymes during development of human masseter muscle. Persistence of developmental isoforms during postnatal stage. Development 108, 239-249.

Szabo G., Dallmann G., Muller G., Patthy L., Soller M. and Varga L. (1998). A deletion in the myostatin gene causes the compact (Cmpt) hypermuscular mutation in mice. Mamm. Genome 9, 671-672.

Sperber G.H. (2001). Craniofacial development. BC Decker. Hamilton, Ontario. pp 171-182

Tzahor E. (2009). Heart and craniofacial muscle development: a new developmental theme of distinct myogenic fields. Dev. Biol. 327, 273-279.

Usami A., Abe S. and Ide Y. (2003). Myosin heavy chain isoforms of the murine masseter muscle during pre- and post-natal development. Anat. Histol. Embryol. 32, 244-248.

van Rooij E., Sutherland L.B, Qi X., Richardson J.A., Hill J. and Olson E.N. (2007). Control of stress-dependent cardiac growth and gene expression by a microRNA. Science 316. 575–579.

Wehling M., Cai B. and Tidball J.G. (2000). Modulation of myostatin expression during modified muscle use. FASEB J. 14, 103-110.

White P., Burton K.A., Fowden A.L. and Dauncey M.J. (2001). Developmental expression analysis of thyroid hormone receptor isoforms reveals new insights into their essential functions in cardiac and skeletal muscles. FASEB J. 15, 1367-1376.

Widmer C.G., English A.W. and Morris-Wiman J. (2007). Developmental and functional considerations of masseter. Arch. Oral Biol. 52, 305-308.

Yamane A., Ohnuki Y. and Saeki Y. (2000). Delayed embryonic development of mouse masseter muscle correlates with delayed MyoD family expression. J. Dent. Res. 79, 1933-1936.

Yasaka N., Suzuki K., Kishioka Y., Wakamatsu J. and Nishimura T. (2013). Laminin binds to myostatin and attenuates its signaling. Anim. Sci. J. 84, 663-668.

Yi M., Chen X., Li Q., An X. and Chen Y. (2009). Effect of thyroid hormone on the gene expression of myostatin in rat skeletal muscle. Asian-Aust. J. Anim. Sci. 22, 275 -281.

Yu F., Göthe S., Wikström L., Forrest D., Vennström B. and Larsson L. (2000). Effects of thyroid hormone receptor gene disruption on myosin isoform expression in mouse skeletal muscles. Am. J. Physiol. Regul. Integr. Comp. Physiol. 278, 1545-1554.

Accepted May 18, 2015